J Mater Sci (2011) 46:2814–2819
DOI 10.1007/s10853-010-5157-1

Study on NbC particulate-reinforced iron matrix composite produced in situ

Lisheng Zhong · Yunhua Xu · Xiaojie Liu · Fangxia Ye

Received: 3 September 2010 / Accepted: 4 December 2010 / Published online: 16 December 2010

Abstract In the infiltration casting process and heat treatment method, gray cast iron and niobium wires are compounded. The reinforcement phase NbC particles are synthesized in situ between niobium wires and graphite phases in the gray cast iron using heat treatment. The microstructure and micro-hardness of the compound region are observed and measured through X-ray diffraction, scanning electron microscopy, and micro-hardness testing. The results indicate that at 1172 °C for 25 min, the in situ reaction area is diffusely extended eight times larger than the original diameter of 0.7 mm. The NbC particles synthesized in situ are tiny square- or rectangle-like particles that are evenly distributed in the gray cast iron. The highest micro-hardness value of the composite region is 1988 $HV_{0.05}$, and the average micro-hardness value of the composite region after 20 min heat treatment is 953 $HV_{0.05}$ or about five times larger than that of the matrix. After heat treatment at 1172 °C for 25 min, the average micro-hardness value of the composite was about 458 $HV_{0.05}$, and the average macro-hardness was 49.2 HRC.

L. Zhong · Y. Xu
School of Material Science and Engineering, Xi'an University of Architecture and Technology, Xi'an 710055, People's Republic of China

L. Zhong · Y. Xu (✉) · X. Liu · F. Ye
Institute of Wear Resistant Materials, Xi'an University of Architecture and Technology, 13 Yanta Road, Xi'an 710055, People's Republic of China
e-mail: xuh_2000@126.com

Introduction

Composite materials with iron and steel matrices and ceramic particle reinforcements provide scope for the production of relatively inexpensive wear-resistant materials. Most studies on iron- and steel-based composites involve TiC, WC, and VC reinforcement, which is introduced into the iron or steel matrix through powder metallurgy (P/M), self-propagation high-temperature synthesis (SHS), various casting techniques, in situ reaction techniques, and so on [1–7]. However, powder metallurgy is based on the addition of ceramic reinforcements to the matrix materials prepared separately before the composite fabrication. This process results in interfacial reactions and poor wettability between the reinforcements and the matrix due to surface contamination of the reinforcements. The particulate-reinforced composite produced by SHS cannot be directly used as structural materials because of its porosity and looseness, making the intrinsic porosity in the reaction process difficult to handle. The particle segregation of reinforcements in the matrix is likely to be uneven using various casting technologies due to the density difference between the matrix and the reinforcement, which is caused by the manufacturing of the particulate-reinforced composite. The volume fraction of the reinforcement is limited because the fluidity of the matrix is reduced at high reinforcement levels. In situ techniques involve a chemical reaction resulting in the formation of a very fine and thermodynamically stable ceramic phase within a metal matrix, which is considered a promising method. The reinforcement–matrix interfaces are clean, thus resulting in a strong interfacial bonding. The distribution of reinforcements in the matrix is uniform, making it useful for better mechanical properties of the composite.

Niobium is an element that has strong affinity with carbon. It cannot be dissolved in the austenite of ferrous alloys even at high temperatures [8]. Moreover, NbC with a high melt temperature of 3600 °C is easily produced in the matrix through in situ reaction. NbC also has high microstructure hardness of 2400 $HV_{0.05}$, making it suitable for the reinforced phase of wear-resistant materials. There are three methods for preparing NbC particle-reinforced composite materials. First, fine powders of NbC are added into the alloy melt to synthesize the composite. Second, alloy and NbC powders are mixed to sinter in the furnace [9]. Third, laser cladding is conducted by adding NbC powders [10]. All these techniques are based on the addition of NbC powders to the matrix materials, which may be in molten or powder form. In this case, the NbC scale that is the reinforcing phase is limited by starting powder size, interfacial reactions between reinforcements and matrix, poor wettability between the reinforcements and the matrix due to surface contamination of the reinforcements, residual porosity, and uneven distribution of the reinforcement. Moreover, the bonding strength of NbC particles with the matrix is usually poor and has small volume fraction. The particle sizes are large, making it difficult and costly to distribute in the matrix.

In this article, infiltration casting and heat treatment are combined. First, niobium microwires are set in the casting pattern using the infiltration casting process in the procedure. Then, niobium wires are reacted in situ with carbon elements in the matrix using heat treatment to form NbC particle-reinforced composite gray cast iron. The possibility of preparing NbC particle-reinforced composite iron by in situ reaction procedure is also discussed in this article. The morphology, size, and distribution behavior of NbC particles are also analyzed.

Experimental procedure

The starting materials were gray cast iron and niobium wires (∅ 0.7 mm) with 99.99% purity. They were utilized as carbon and niobium sources for the in situ synthesis of niobium carbides within the iron matrix. The chemical composition (wt%) of the gray cast iron was Fe–4.22C–0.58Si–0.268Mn–0.224P–0.024S. According to the DSC results, the sectioned samples were subjected to heat treatment at 1172 °C at different times (0, 15, 20, and 25 min) in a horizontal tube furnace with a modest flow of argon and cooled down naturally to room temperature.

After being polished with diamond paste and etched with a 4% Nital solution, the microstructure of the specimens was examined using a JSM-5800 scanning electron microscope (JEOL, Japan) equipped with an energy dispersive X-ray spectroscopy (EDS). The X-ray diffraction (XRD) data were recorded on a PW 1730 X-ray diffractometer (Philips, The Netherlands) with monochromated CuKα radiation at 40 kV and 40 mA in the 2θ range of 10°–90°. Micro-hardness of the specimens was measured using a HDX-1000 digital micro-hardness tester consisting of a square-based pyramidal diamond indenter with a 136° angle between two opposite faces. The static load was 50 g, and the dwell time of loading was 15 s. An average micro-hardness value was taken from at least five different measurements. To determine the pouring temperature of the gray cast iron melt, DSC/TGA analysis was performed on a Q600 SDT (TA Instruments, USA) for the sample with a diameter of 2 mm and a length of 2.6 mm, which was prepared using gray cast iron and niobium wire. The specimen was heated at 10 °C/min up to a maximum temperature of 1400 °C with a 150 mL/min flow rate of argon gas and cooled down to room temperature.

Results and discussion

Figure 1 is the DTA curve of the sample displaying three endothermic peaks at 738, 814, and 1172 °C and an exothermic peak at 1280 °C. The endothermic peak at 738 and 814 °C arises from the grain boundary dissolution and allotropic change $\alpha \rightarrow \gamma$ [9]. The third endothermic peak (maxima at 1172 °C) is thought to arise from eutectic reactions $L \rightarrow \gamma + G + NbC$. The exothermic peak at 1280 °C is attributed to the formation of niobium carbides by the reaction $L \rightarrow \gamma\text{-Fe} + NbC$ [10]. The reaction taking place near the ternary eutectic transformation is conducive to the precipitation of graphite and is beneficial for the maintenance of matrix consistency. From the DSC results, 1172 °C was determined to be the optimum temperature for heat treatment.

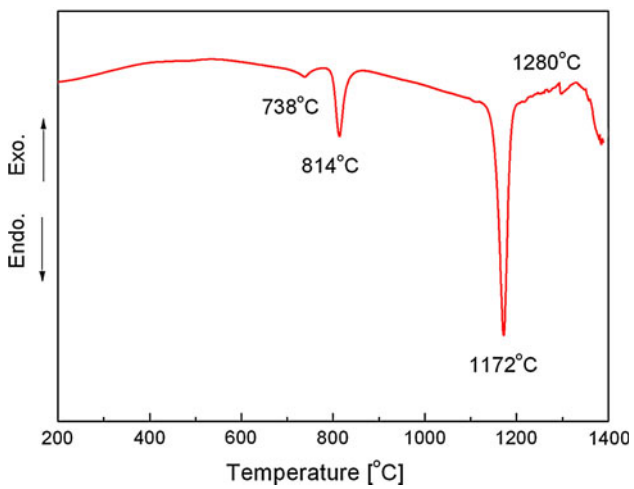

Fig. 1 DSC curve of the specimen

The microstructure of the niobium carbide particulate-reinforced metal matrix composite is shown in Fig. 2a. Many tiny square- and rectangle-like particles can be found in the matrix. The results of the microanalysis of both tiny square- and rectangle-like particles are presented in Fig. 2b. The EDS result in Fig. 2b shows that the tiny square-like particles consist of a high percentage of Nb (47.47 atom %) and C (51.49 atom %). Meanwhile, the rectangular particles have Nb (48.63 atom %) and C (51.10 atom %) as major elements. The remaining particles were the rare element Fe. These white particles are evidently rich in Nb and C. The XRD patterns of the products also demonstrated that the NbC phase could be synthesized in situ through the present technique, as shown in Fig. 3d. The above analysis showed that the tiny square- and rectangle-like phases were all comprised of NbC.

To study the process and formation of niobium carbide particulate-reinforced metal matrix composites, samples under heat treatment in different times are studied.

Figure 3 indicates the XRD patterns of niobium carbide particulate-reinforced metal matrix composites heat treated at 1172 °C for 0, 15, 20, and 25 min. The presence of G (graphite), α-Fe, Nb, and NbC for composition with 0, 15, and 20 min heat treatment and the presence of G (graphite), α-Fe, and NbC for composition with 25 min heat treatment were detected. With the increase of heating time, the Nb peak intensity decreased, the NbC peak intensity increased, and the Fe peaks were relatively unchanged. The sudden disappearance of niobium diffraction peaks after heat treatment at 1172 °C for 25 min confirmed that all niobium atoms were consumed by reacting with graphite in the matrix and that only a small amount of non-reacted graphite remained. Moreover, only two phases (i.e., NbC and ferrite) and niobium carbide-dominated metal matrix composites can be obtained under the current conditions along with a small amount of non-reacted graphite.

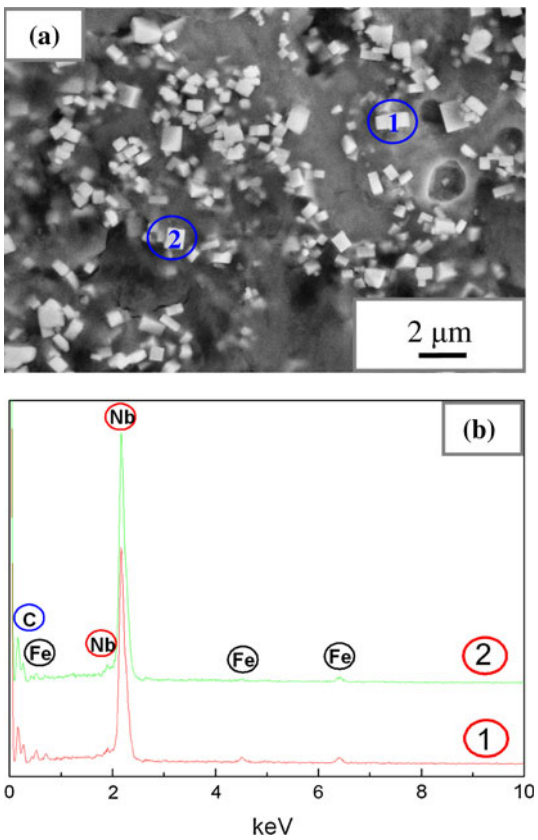

Fig. 2 SEM micrographs (**a**) and EDS patterns (**b**) of tiny square- and rectangle-like particles of the Fe–NbC composite

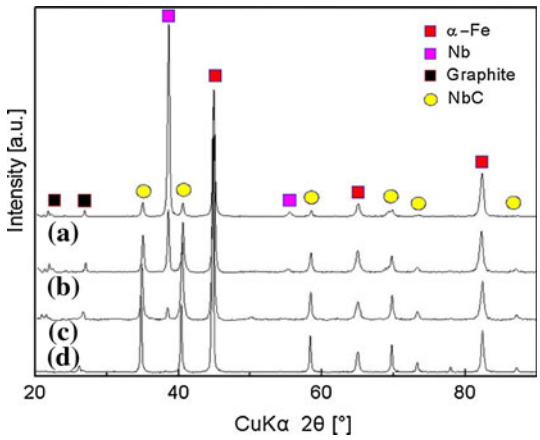

Fig. 3 XRD patterns of the niobium carbide particulates-reinforced metal matrix composites heat treated at 1172 °C for 0 (*a*), 15 (*b*), 20 (*c*), and 25 min (*d*)

Figure 4a–d shows the microstructure of the cross section of the composite in the zone of the in situ niobium wire reaction after heat treatment for 0, 15, 20, and 25 min, respectively. The results indicate that the diffused region gradually increased with the reaction time. The niobium phase disappeared after heat treatment for 25 min. Figure 4d shows the microstructure of the composite in the zone of in situ Nb wire reaction after heat treatment at 1172 °C for 25 min. The results indicate that the in situ reaction was complete for niobium wire and that the niobium phase had already disappeared. The reaction occurred around the niobium wire through the heat diffusion of niobium elements. The diameter of the reaction zone was extended to 2.1 mm compared to the 0.7-mm diameter of the original niobium wire. The reaction area was eight times larger than that of the original niobium wire area. The original boundary also disappeared without any defects. The product density gradually decreased from the center of the in situ reaction zone to the boundary. The NbC particles synthesized in situ were tiny square- or rectangle-like particles 0.2–1.0 μm in size and distributed evenly in the gray cast iron. However, the number of tiny

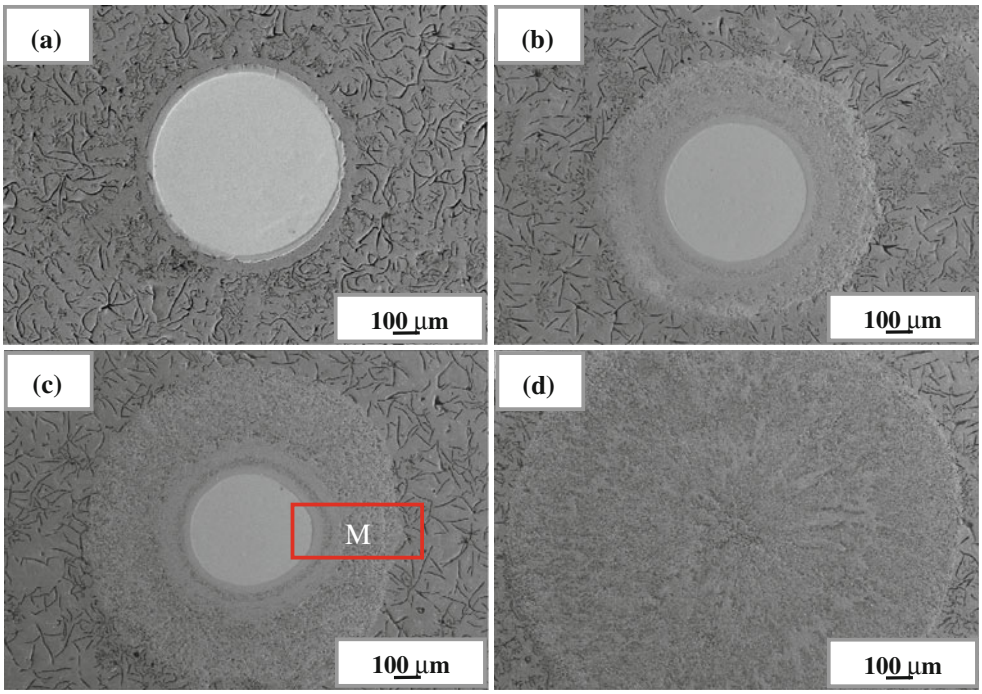

Fig. 4 Cross section of the niobium carbide particulates-reinforced metal matrix composites heat treated at 1172 °C for 0 (**a**), 15 (**b**), 20 (**c**), and 25 min (**d**). (SEM micrographs)

square- and rectangle-like particles decreased and the size slightly increased. Plate-like graphite could be observed near the boundary of the reaction. Careful examination of the matrix indicated that it was ferrite phase.

After heat treatment, the composite region can be divided into three apparent concentric circles (regions) between the niobium wire and the iron matrix. The three regions are labeled A, B, and C where the diffusion reaction has taken place. To obtain more information on the regions (A, B, and C) formed after the in situ reaction, scanning electron microscopy (SEM) was applied of the specimen after heat treatment for 20 min. The SEM micrographs are presented in Fig. 5. Based on the XRD results, the microstructures of regions A, B, and C indicate the presence of tiny square- and rectangle-like particles in the iron matrix. The crystalline NbC particles were uniformly dispersed in the iron matrix in regions A, B, and C. A statistical analysis about the distribution of the dimensions in the different zones was performed, and the results showed that the particle sizes of NbC were 0.2–0.5, 0.3–0.7, and 0.3–1.0 μm in regions A, B, and C, respectively. The particles sizes after 25 min were between 0.4 and 2.0 μm. This indicates that the NbC crystallites grew with the prolongation of heat treatment time.

The micro-hardness distribution in the composite region of the as-prepared composites heat treated at 1172 °C for 20 min is plotted in Fig. 6. As shown in the figure, the highest value (1988 $HV_{0.05}$) was obtained from the diffusion reaction in region A due to intensive NbC. There was a sharp decrease between regions A and B which gave a micro-hardness value of around 402–497 $HV_{0.05}$. Micro-hardness values again increased when it entered region B, with the trend subsequently falling to 412 $HV_{0.05}$ in region C. The micro-hardness values were a little different in regions B and C due to the presence of NbC crystallites. This can be attributed to the formation of NbC particles, that is, in region B, the NbC particles were formed with highly agglomerated morphology while the NbC particles were formed separately in the iron matrix in region C. We assumed that indentation in region C might occur randomly either on a smaller NbC particle or directly on the iron matrix, giving lower micro-hardness values.

The main reason the micro-hardness value sharply decreased between regions A and B could be the presence of an enrichment iron zone, as shown in Fig. 5a. The surface scan results between regions A and B were shown in Fig. 7. According to it, there is a narrow rich iron and poor Nb zone between region A and B. In this zone, the micro-hardness sharply decreased (Fig. 6). The presence of such a zone cannot be explained by the authors and needs an in-depth study. The average hardness value of the composite region (regions A, B, and C) was 953 $HV_{0.05}$ at 1172 °C for 20 min, and the micro-hardness of the niobium wire and iron matrices were 383 and 195 $HV_{0.05}$, respectively. The average value of the composite region is five times higher than that of the iron matrix and two times

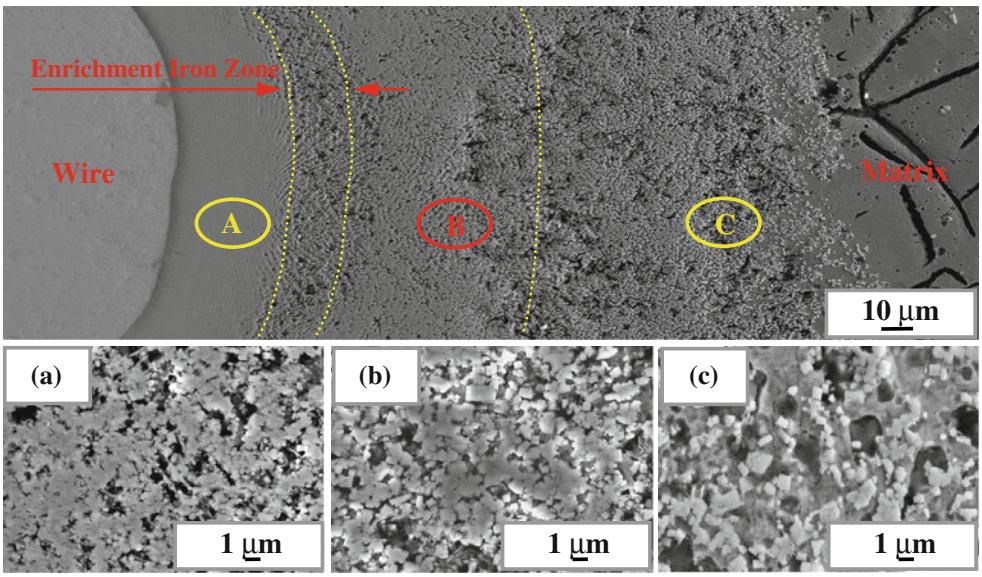

Fig. 5 Enlarged SEM micrographs of region M in Fig. 5 and region *A* (**a**), region *B* (**b**), and region *C* (**c**) of the specimen heat treated at 1172 °C for 20 min

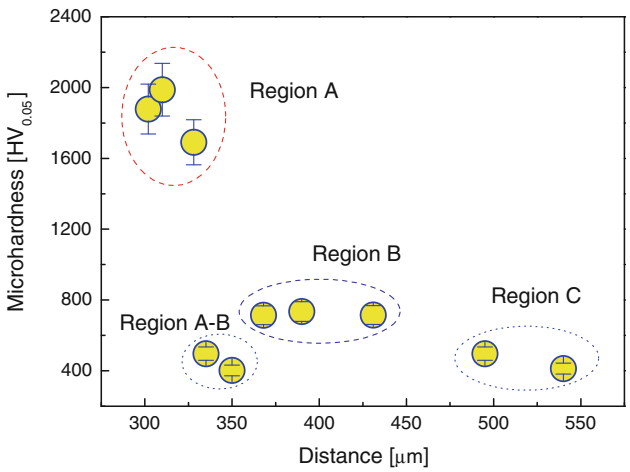

Fig. 6 Micro-hardness distribution in the composite region of the specimen heat treated at 1172 °C for 20 min as a function of a distance from the center of reinforcement phase to the iron matrix

higher than that of the niobium wires. After heat treatment at 1172 °C for 25 min, the average micro-hardness value of the composite was about 458 $HV_{0.05}$, and the average macro-hardness was 49.2 HRC. Both were the average of five measurements.

The following possible reaction may occur in the Fe–Nb–C system:

$$\mathrm{Nb(s)+C(s)=NbC(s)} \quad \Delta G_1 = -182.330 + 0.10052T$$
$$\mathrm{2Nb(s)+C(s)=Nb_2C(s)} \quad \Delta G_2 = -262.294 + 0.25815T$$
$$\mathrm{3Fe(s)+C(s)=Fe_3C(s)} \quad \Delta G_3 = 26.690 + 0.24800\,T,\ (190\text{–}842\,^{\circ}\mathrm{C})$$
$$\Delta G_3 = 10.350 - 0.01027T,\ (842\text{–}1535\,^{\circ}\mathrm{C})$$

Figure 8 plots the Gibbs free energy of NbC, Nb_2C, and Fe_3C as a function of temperature according to the reaction equations above. The Gibbs free energy of Nb_2C at 1172 °C had a positive value and NbC and Fe_3C had negative values, illustrating the non-formation of Nb_2C and the existence of NbC and Fe_3C. However, at the reaction temperature of 1172 °C, ΔG_3 was only slightly negative with a value of −1.67 kJ/mol. Hence, NbC was the most thermodynamically favored product compared with Fe_3C.

Conclusion

Using a novel process combining infiltration casting process technology with heat treatment, the production of an iron matrix composite reinforced with NbC particulate is feasible. The required bonding strength is satisfied due to the in situ reaction. The produced NbC particles are tiny square- and rectangle-like particles 0.2–1.0 μm in size. The in situ reaction area is diffusely extended to eight times larger than the original diameter of 0.7 mm after being kept in 1172 °C for 25 min. The highest micro-hardness value of the composite region after being kept for 20 min is 1988 $HV_{0.05}$ and the average micro-hardness value is 953 $HV_{0.05}$, which is about five times that of the matrix. After heat treatment at 1172 °C for 25 min, the average micro-hardness value of the composite was about 458 $HV_{0.05}$, and the average macro-hardness was 49.2 HRC.

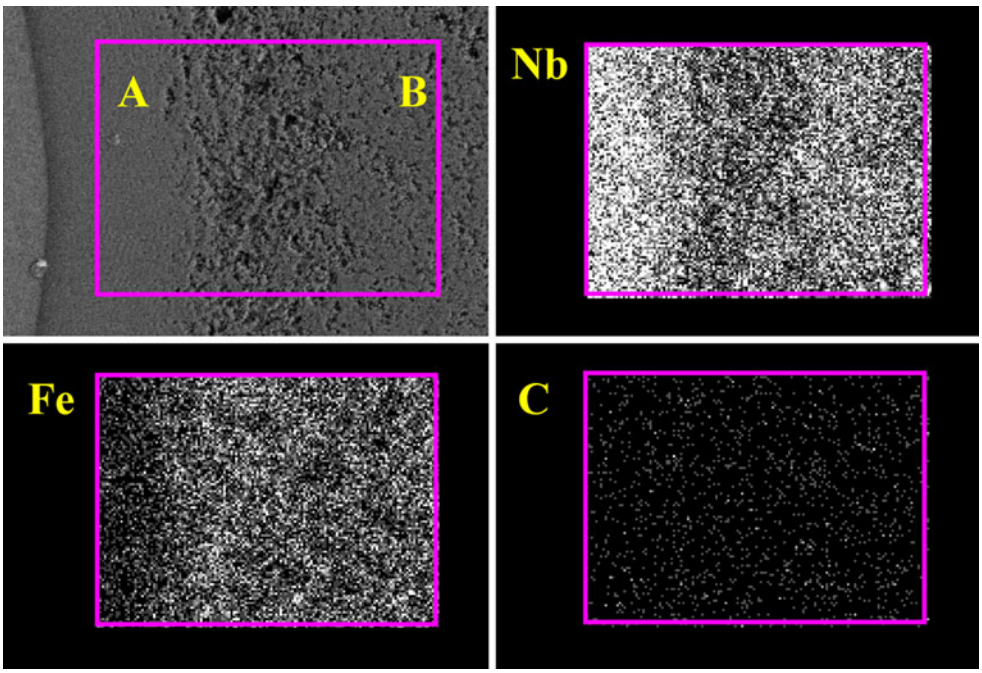

Fig. 7 The surface scan results between regions *A* and *B*

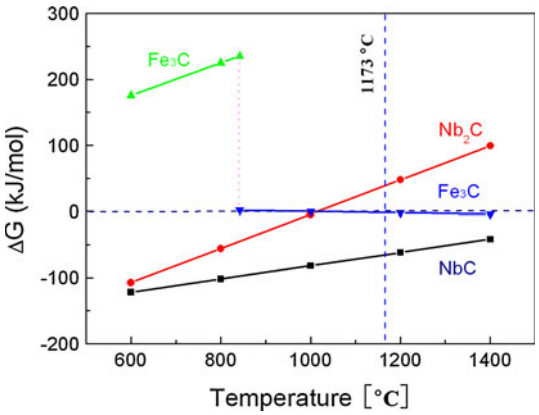

Fig. 8 Gibbs free energies for Nb_2C, NbC and Fe_3C (Fe_3C at low temperature indicated under 842 °C and at high temperature above 842 °C) as a function of temperature

Acknowledgements This study was granted by the National High Technology Research and Development Program ("863" Program) of China (No. 2008AA03Z310). At the same time, the authors acknowledge the financial support from the National Natural Science Foundation of China (No. 50974101).

References

1. Sun GJ, Wu SJ, Su GC (2010) Wear 269:285
2. Feng K, Hong M, Yang Y, Wang W (2009) Int J Refract Met Hard Mater 27:852
3. Kim HJ, Lee CH, Hwang SY (2005) Surf Coat Technol 191:335
4. Mei Z, Yan YW, Cui K (2003) Mater Lett 57:3175
5. Zhou R, Jiang Y, Lu D (2003) Wear 255:134
6. Wang Y, Sun Z, Ding Y, Li F (2004) Mater Des 25:69
7. Wang J, Wang Y, Ding Y, Gong W (2007) Mater Des 28:2207
8. Mathon M, Connétable D, Sundman B, Lacaze J (2009) Calphad 33:136
9. Thümmler F, Gutsfeld C (1991) Powder Metall 23:285
10. Ebner R, Kriszt B (1992) In: Proceedings of the 4th European Conference on Laser Treatment of Materials, Göttingen, pp 187–192